Raman Scattering as a Probe of Crystallinity in PTCDA and H_2Pc Single-Layer and Double-Layer Thin Film Heterostructures

S. Heutz,[†] G. Salvan,[‡] S. D. Silaghi,[‡] T. S. Jones,*[,†] and D. R. T. Zahn[‡]

Centre for Electronic Materials and Devices, Department of Chemistry, Imperial College, London SW7 2AZ, U.K., and Halbleiterphysik, Technische Universität Chemnitz, D-09107 Chemnitz, Germany

Received: July 30, 2002

The vibrational properties of single-layer PTCDA (perylene-3,4,9,10-tetracarboxylic dianhydride) and H_2Pc (metal-free phthalocyanine) thin films and PTCDA-H_2Pc double-layer heterostructures are studied by Raman scattering. The evidence of crystallinity of the single-layer films can be supported by the existence of phonons, as well as polarization dependence. Resonance enhancement Raman scattering has been used to selectively measure the individual layer properties in double-layer H_2Pc/PTCDA and PTCDA/H_2Pc heterostructures. When H_2Pc is grown on PTCDA, its structure departs from the herringbone arrangement characteristic of unstrained H_2Pc films, as demonstrated by the different peak intensities in the Raman spectra. Well-defined phonons and the polarization dependence in the H_2Pc top layer are characteristic of long-range order, indicating that the H_2Pc molecular planes in the templated structure are crystalline. No evidence for a new structure was observed for PTCDA deposited on top of a H_2Pc first layer. Here, the relative intensity of the phonons in the PTCDA top layer demonstrates that the PTCDA forms microcrystallites due to strain at the molecular heterojunction, before relaxing to its bulk crystalline form.

1. Introduction

Molecular thin films are attracting increasing interest as cheap and versatile components for a wide range of electronic and optoelectronic devices.[1] Over the past few years, research has spanned from highly ordered crystalline layers to amorphous materials, and increasingly complex architectures are being studied to improve device performance.[2] Molecular heterostructures form the basis of several devices including organic light emitting diodes and solar cells. A more detailed understanding of the properties of heterostructures will lead to improved device design and performance.

Perylene-3,4,9,10-tetracarboxylic dianhydride (PTCDA) and metal-free phthalocyanine (H_2Pc) are two materials that have been commonly used in molecular device applications. Indeed, PTCDA and Pc formed the basis of the first double-layer solar cell.[3] The properties of the individual single-layer components have been studied extensively; however, there have been very few studies on double-layer structures based on these types of materials. Recently, we have shown that significant interactions can occur between double-layer structures containing PTCDA and H_2Pc, with the properties of the second layer showing significant structural and morphological changes when compared to the corresponding single-layer films.[4−6] This observation was based on X-ray diffraction (XRD) and atomic force microscopy (AFM) studies.

Raman spectroscopy has been applied successfully in the study of the structural properties of molecular thin films, with porphyrins being one of the earliest compounds studied.[7] Aroca et al. pioneered Raman investigations on Pc derivatives, studying the effects of metal nanoclusters[8,9] and excitation wavelength[10] on the Raman intensities. Studies of molecular orientation by Raman have been limited to metal Pcs and utilize the effects of polarization. Internal vibrations of the molecule provide information about the orientation of the molecules relative to the substrate[11,12] for thicknesses down to one monolayer,[13] and relaxation of the structure can also be probed.[14] For thicker films where the crystal structure is well-known, it is also possible to study the orientation of the crystallites using the symmetry of the external crystal modes.[15] Identification of different polymorphs is not straightforward, but recent work has shown that it is possible to identify α and β-H_2Pc thin films by focusing on specific regions of the vibrational spectrum.[16] Infrared and Raman have also been used to study PTCDA both in the bulk[17,18] and in thin films.[19,20] The experimental data was analyzed using known perylene vibrations and density-functional tight binding (DFTB) calculations on both single molecules and dimers,[21] so that complete assignments have been achieved. Recently, Kam et al. applied Raman to the study of mixed molecular systems and achieved a partial selectivity to perylene and phthalocyanine derivatives.[22]

In this paper, we present results from a Raman study of both H_2Pc and PTCDA single-layer structures and double-layer H_2Pc/PTCDA and PTCDA/H_2Pc heterostructures. The Raman results confirm the structural disruption of a H_2Pc layer deposited on a PTCDA first layer and show that PTCDA grows as strained microcrystals on a H_2Pc first layer, before subsequently relaxing to its bulk structure.

2. Experimental Details

The films were grown by organic molecular beam deposition in an ultrahigh vacuum chamber with a base pressure of 2×10^{-9} mbar. The glass substrates were cut from microscope slides (BDH superpremium), cleaned in a methanol sonic bath, and dried under a stream of dry nitrogen. H_2Pc (Syn Tech, 98%)

* To whom correspondence should be addressed. Phone: +44 (0) 20 7594 5794. Fax: +44 (0) 20 7594 5801. E-mail: t.jones@imperial.ac.uk.
[†] Centre for Electronic Materials and Devices.
[‡] Halbleiterphysik.

10.1021/jp0266392 CCC: $25.00 © 2003 American Chemical Society
Published on Web 03/29/2003

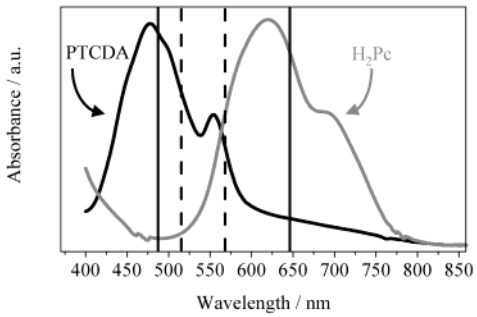

Figure 1. Absorption spectra of 60-nm PTCDA and 60-nm H_2Pc single-layer films, with the wavelengths of the laser lines studied indicated by solid and dashed vertical lines. The Raman excitation using the wavelengths indicated by solid lines produces signals which are selective to each material.

and PTCDA (Lancaster, twice sublimed) were outgassed under vacuum for 5 h prior to deposition, and evaporated from two separate sources, held at 320 and 330 °C, respectively. The growth rate was ~10 nm/min, as determined by a quartz crystal microbalance positioned near the substrate. The thickness of the individual layers was 60 nm unless otherwise stated, corresponding to a total film thickness of 120 nm for the double-layer structures. The substrates were maintained at room temperature during film growth.

The growth chamber was integrated in an in situ Raman setup in the so-called macro configuration. Excitation was obtained from a Kr^+ laser (Coherent Innova 300) for lines at 647.1 nm (1.92 eV) and 568.2 nm (2.28 eV), or from an Ar^+ laser (Coherent Innova 70) that produces lines at 488.0 and 514.5 nm (2.54 and 2.41 eV). The incoming beam, usually held at a power of ~10−20 mW, was focused to a spot of about 300 μm in diameter and strikes the sample at an angle of 30° with respect to the surface normal. The light scattered perpendicular to the substrate plane was collected by a Dilor XY triple monochromator with a multichannel charge coupled device detector. The spectral resolution spanned from ~3.3 cm^{-1} for excitation at 488.0 nm, to ~2 cm^{-1} for excitation at 647.1 nm, as determined by the full width at half-maximum of the laser line for a typical slit width of 200 μm.

Raman studies were also carried out ex situ in a micro configuration using an Olympus BH-6 microscope. This experimental setup realizes a backscattering geometry, with both the incident beam and the scattered beam passing through the microscope objective which was kept at 100 times magnification. To avoid any degradation of the films in this configuration, the incident power was reduced to 2 mW.

3. Results and Discussion

Figure 1 shows the absorption spectra for single layers (60 nm) of H_2Pc and PTCDA grown on glass substrates at room temperature. As expected from these growth conditions, the absorption of H_2Pc is characteristic of the α polymorph, with the film containing small spherical crystallites.[16,23,24] PTCDA also forms crystalline single layers, with the (102) plane nearly parallel to the substrates. The crystallinity of the two single layers was confirmed by powder X-ray diffraction. Although both materials absorb in the 500−600-nm region, specific absorption is displayed at shorter or longer wavelengths for PTCDA or H_2Pc, respectively. It can be expected therefore that selective enhancement of the Raman signal can be produced by each material through resonance with a specific electronic transition. A range of wavelengths spanning the electronic absorption spectra have hence been probed: blue (Ar^+ 488.0 nm), green (Ar^+ 514.5 nm), yellow (Kr^+ 568.2 nm), and red (Kr^+ 647.1 nm), as shown by the vertical lines in Figure 1.

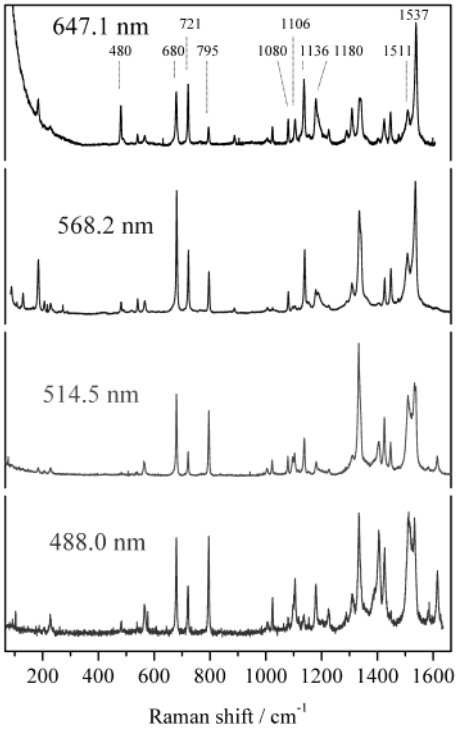

Figure 2. Raman spectra of 60-nm-thick α-H_2Pc films measured in the micro configuration, taken at four different laser wavelengths. Valuess in small fonts indicate vibration frequencies.

3.1. H_2Pc Single Layers. The isolated H_2Pc molecule has D_{2h} symmetry, and the normal modes are distributed into 29 A_g, 13 B_{1g}, 14 B_{2g}, and 28 B_{3g} Raman active modes, with 28 B_{1u}, 28 B_{2u}, and 15 B_{3u} infrared (IR) active modes. Since the α-H_2Pc crystals belong to the C_{2h} space group with two molecules per unit cell, insertion in the crystal lattice leads to 84 A_g and 84 B_g Raman modes (due to Davydov splitting).

Sixty-nanometer-thick α-H_2Pc films were first measured ex situ using the micro-Raman configuration, and the influence of excitation wavelength was investigated (Figure 2). The four wavelengths used (488.0, 514.5, 568.2, and 647.1 nm) span the electronic spectrum of α-H_2Pc, from the Soret or B-band to the maximum of the Q-band. The absolute intensities of the vibrational peaks should be considered with care. In Figure 2, the spectra all have similar signal-to-noise ratios, even though excitation at wavelengths corresponding to high electronic absorption should lead to more effective overall enhancement. The apparent identical Raman cross-section is due to the spectrometer response, which is diminished by a factor of 5 when the measured wavelength decreases from 647.1 to 488.0 nm.

The spectra were fitted using Lorentzian peak shapes, and it was found that the peak positions and full widths at half-maximum (fwhm) are not affected by the excitation wavelength. The main lines for excitation at 647.1 nm, with their intensity normalized to the most intense vibration at 1539 cm^{-1}, are listed in Table 1 and correspond well to literature values.[10] However, the intensity ratios of the peaks are very sensitive to the excitation wavelength, indicating that resonance enhancements play an important role. To compare the peaks, all intensities for the different excitation wavelengths were normalized to a vibration that is unaffected by resonance. The stretching mode at 1340 cm^{-1} has been used as a reference since it shows a

TABLE 1: Raman Modes Observed with Excitation at 647.1 nm in 60-nm-Thick H_2Pc Single Layers Deposited on Glass and in 60-nm H_2Pc Layers Deposited on Top of a PTCDA Template Layer[a]

	H_2Pc single layer		H_2Pc in PTCDA/H_2Pc	
wavenumber/cm^{-1}	relative intensity (unpolarized)	ρ_p	relative intensity (unpolarized)	ρ_p
480	0.25	0.66	0.24	1.2
680	0.41	0.81	0.36	0.61
721	0.36	0.81	0.41	0.87
795	0.11	0.78	0.05	0.62
1080	0.13	0.77	0.13	1.6
1104	0.23	0.75	0.27	1.4
1140	0.36	0.85	0.25	0.67
1180	0.37	0.88	0.46	1.4
1197	0.12	0.84	0.20	1.7
1227	0.08	0.82	0.18	1.5
1290	0.11	0.81	0.22	1.5
1309	0.36	0.84	0.54	1.1
1340	0.42	0.75	0.28	0.73
1424	0.27	0.91	0.34	2.2
1447	0.27	0.87	0.31	1.0
1511	0.67	0.72	0.56	0.97
1533	0.59	0.65	0.96	0.69
1539	1.00	0.81	1.00	0.56

[a] Depolarization ratios, ρ_p, and relative intensities (normalized to the most intense mode at ~1539 cm^{-1} in both cases) are listed.

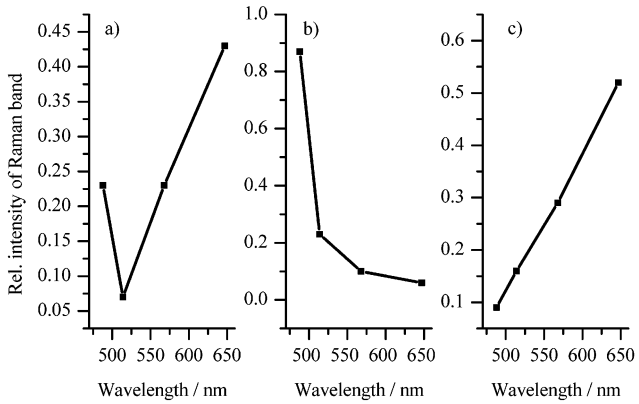

Figure 3. Relative intensity of Raman bands for 60-nm α-H_2Pc films as a function of laser wavelength (488.0, 514.5, 568.2, and 647.1 nm), normalized to the vibration at 1340 cm^{-1}. Three different trends are observed, and are represented by the vibrations at (a) 721 cm^{-1}, (b) 1406 cm^{-1}, and (c) 1140 cm^{-1}.

maximum in the preresonance region (i.e., when the H_2Pc film is excited at 514.5 nm). It is a more appropriate choice for identification of resonance trends than normalizing to the most intense mode at 1539 cm^{-1}, which is affected by the excitation wavelength. The intensity profiles shown in Figure 3 for the vibrations at 721, 1406, and 1140 cm^{-1} are representative of three clear different trends: the relative intensity shows a valley in the preresonance region, indicating that the vibrations involved are enhanced by both the Soret band and the Q-band (480, 680, 721, 1104, 1180, 1533, and 1539 cm^{-1}), the intensity decreases when the laser wavelength is increased, and resonance with the Soret band is the dominant mechanism (566, 795, 1406, and 1511 cm^{-1}), the relative intensity increases with the laser wavelength, and resonance with the Q-band is predominant (1080 and 1140 cm^{-1}).

It has been shown that the electron density involved in the Q-band transition is localized on the macrocycle, whereas the B-band affects the benzene rings.[25] It is possible therefore to correlate the intensity profile of the bands with the localization of the corresponding vibrations involved. Peaks following case a (Figure 3a) involve vibrations on bonds common to the benzene ring and the macrocycle (e.g., at 1533 cm^{-1}, which involves stretching of the C−C bond common to the pyrrole and benzene units) or are very delocalized (e.g., breathing or deformation of the macrocycle at 680 and 721 cm^{-1}), respectively. Case b (Figure 3b) is followed by benzene ring deformations (566 cm^{-1}) or isoindole ring stretching modes (1406 cm^{-1}), where the largest displacement is on the benzene moieties. As expected, the localized pyrrole breathing mode at 1140 cm^{-1} follows case c, Figure 3c.[10]

Two mechanisms can lead to resonance enhancement.[26] The totally symmetric modes are enhanced by the A term due to Franck−Condon overlap, while coupling between closely spaced excited electronic levels leads to enhancement of nontotally symmetric modes via the B term.[27] Aroca et al.[10] argued that totally symmetric vibrations should follow the intensity profiles (a) and (b), based on work carried out on porphyrins. B term enhancement is also likely since the two electronic levels involved in the Q or B band can easily lead to coupling. The symmetry of the enhanced modes can be estimated by calculating the $\langle s|\partial H/\partial Q|e\rangle$ integral dominating the B term, where s and e are two closely spaced electronic levels, and H is the electronic Hamiltonian which depends on the atomic coordinates Q. For coupling between the Q_x and Q_y transitions which have B_{2u} and B_{3u} symmetry, respectively, the B_{1g} modes are enhanced. In the case of coupling within the Soret band, where the two B-band transitions are A_u and B_{3u}, the B_{3g} modes would be enhanced. In conclusion, vibrations enhanced by excitation into the Soret band can be either A_g or B_{3g}, whereas both the A_g and B_{1g} modes are enhanced through resonance with the Q-band.

The effect of polarization on the 60-nm thick H_2Pc films was also analyzed in the backscattering geometry with the incident and scattered light in parallel and crossed polarization. Polarization has no influence on the peak positions and widths, but it does affect the intensity ratios. The depolarization ratios ρ_p, corresponding to the ratio of peak intensities observed in parallel and crossed polarization, have been calculated for H_2Pc, and the values for the most intense vibrations are summarized in Table 1. The polarization dependence is further indication that the molecules have a well-defined orientation in the film.

In situ Raman scattering allowed identification of the low-frequency vibrations, or phonon modes in the H_2Pc films. There are two translationally, nonequivalent molecules in a monoclinic α- or β-H_2Pc crystal, although by convention the α phase is usually defined with a unit cell encompassing four molecules. The space group is C_{2h} and the Raman active rotational phonons are $3A_g + 3B_g$. Figure 4 shows Raman spectra recorded at 647.1 and 568.2 nm, and Table 2 summarizes the position and depolarization ratios of the phonons. Five vibrations appear clearly for both excitations at 33, 41, 55, 72, and 88 cm^{-1}. The higher frequency mode is very intense and in principle could be assigned to an internal vibration. For example, out-of-plane deformations of the macrocycle have been assigned by Aroca et al. at 92 and 133 cm^{-1}.[10] However, ab initio calculations[28,29] indicate no internal vibrations below 90 cm^{-1}, and we therefore assign the peak at 88 cm^{-1} to a phonon mode. An additional weak phonon mode also appears at 26 cm^{-1} when excited at 568.2 nm, leading to the expected six phonon modes. Since the lattice vibrations in a well-ordered crystal are not isotropic, they should be influenced by the polarization of the light. It is clear in Figure 4 that this is the case for α-H_2Pc films. For example, with 647.1-nm excitation, the relative intensity of the modes at 33 and 41 cm^{-1} is inverted when the polarization is changed,

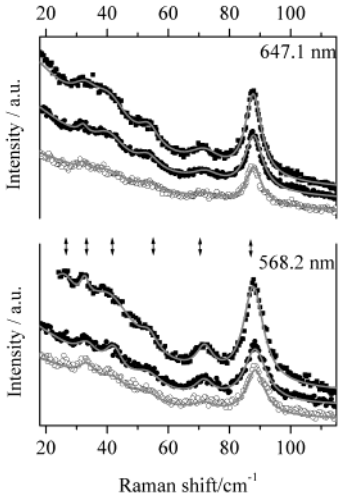

Figure 4. Raman spectra showing the phonons of a H_2Pc film excited with a 647.1 and 568.2-nm laser in (■) unpolarized light, (●) parallel, and (○) crossed-polarized light. The continuous lines are the fitted curves of the phonons and internal modes based on Lorentzian peak profiles.

TABLE 2: Position and Depolarization Ratios, ρ_p, of H_2Pc Films Deposited on Glass and on a PTCDA First Layer[a]

H_2Pc single layer		H_2Pc in PTCDA/H_2Pc	
position/cm^{-1}	ρ_p	position/cm^{-1}	ρ_p
26		30	1.0
33	1.1	37	1.4
41	0.6	43	0.6
54	0.7	54	1.5
72	0.8	71	1.3
88	1.0	88	1.0

[a] The spectra were taken with excitation at 647.1 nm in the micro configuration.

and the vibration at 72 cm^{-1} is particularly weak in crossed polarization at 568.2-nm excitation. The presence of the six phonon modes and their polarization behavior both highlight the good crystalline quality of the H_2Pc films and demonstrate how Raman spectroscopy can be used as a structural probe of thin molecular films.

3.2. PTCDA Single Layers. The choice of laser lines to study Raman scattering in PTCDA films is not as wide as for H_2Pc. The scattering cross-section for nonresonant conditions is very small, so that no signal is detected using a laser wavelength of 647.1 nm. Excitation at 514.5 and 568.2 nm leads to strong photoluminescence, masking any Raman peaks. Hence, all studies were performed with the Ar^+ laser line at 488.0 nm, lying in the absorbance band, but producing only a weak luminescence background.

PTCDA has D_{2h} symmetry and contains 108 internal vibrational modes, of which 54 are Raman active: $19A_g + 18B_{1g} + 10_{2g} + 7B_{3g}$. After examination of the electronic levels, it can be seen that coupling between electronic transitions is excluded, and resonance enhancement occurs only via the A term. Hence, the most intense vibrations are the totally symmetric A_g modes, as demonstrated theoretically.[21] The Raman spectrum acquired from a 60-nm-thick PTCDA film deposited on glass is presented in Figure 5a and corresponds well to literature data.[19] The Raman intensity saturates at very small film thickness (~10 nm) due to the high absorption coefficient of PTCDA for both the incoming and the scattered light.

In contrast to H_2Pc films, the Raman spectra obtained from PTCDA films are independent of sample position, beam and analyzer configuration, and polarization. Since the A_g modes measured have tensor components in both diagonal and nondiagonal positions, the similarity of these components would explain the lack of any change in the internal vibrations. In thin films, Davydov splitting has been observed for the C−O vibration at 233 cm^{-1}.[30] The inset of Figure 5 shows that the mode at 233 cm^{-1} can be deconvoluted into its two Davydov components, leading to a splitting of ~5.2 cm^{-1}. This value corresponds well to the reported literature value of 3.3 cm^{-1} for PTCDA single crystals[17] and 4.9 cm^{-1} for thin films grown on sulfur passivated GaAs (100).[30] Moreover, the line shape is different in crossed and parallel polarization, giving further evidence that this mode is related to the crystallinity of the film.

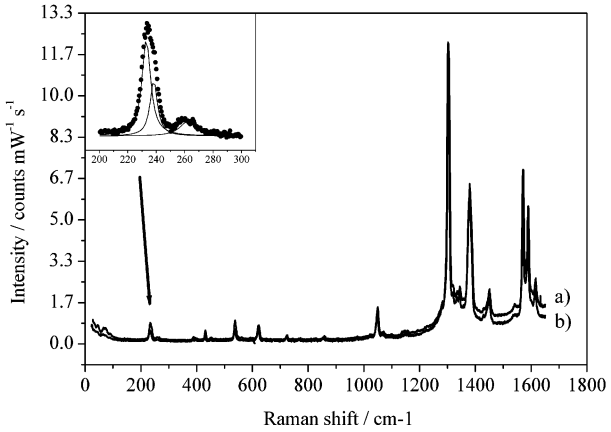

Figure 5. Internal modes of (a) a PTCDA film on a glass substrate and (b) on a 60-nm-thick H_2Pc first layer, taken with macro-Raman and excited at 488.0 nm. The inset shows the Davydov splitting for the C−O vibration of the PTCDA single layer at ~233 cm^{-1}.

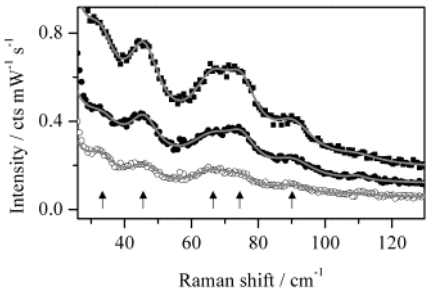

Figure 6. Phonon modes of a 60-nm-thick PTCDA single layer excited with a 488.0-nm laser in (■) unpolarized, (●) parallel, and (○) crossed-polarized configuration. Superimposed are the fitted curves of the phonons, based on Lorentzian peak profiles.

Six rotational optical phonons ($3A_g + 3B_g$) are Raman-active and are expected between ~30 and ~100 cm^{-1}.[17] Figure 6 shows resonance Raman spectra recorded with 488.0 nm excitation on a 60-nm-thick PTCDA film and indicates five well-resolved bands at 34, 46, 67, 74, and 89 cm^{-1}; only the band predicted at 100 cm^{-1} cannot be detected. The observation of the phonon modes in the thin film suggests good crystallinity, which is further supported by their clear polarization dependence (Figure 6, filled and open circles).

3.3. Double-Layer Heterostructures. Raman spectroscopy was used to investigate the vibrational properties of double-layer structures based on successive layers of H_2Pc and PTCDA deposited at room temperature, each layer being 60-nm thick. From the single-layer studies, it has been found that although the two intermediate excitation frequencies (514.5 and 568.2 nm) give signals for both materials, complete selectivity can be obtained with the red and blue lines. It is therefore easy to

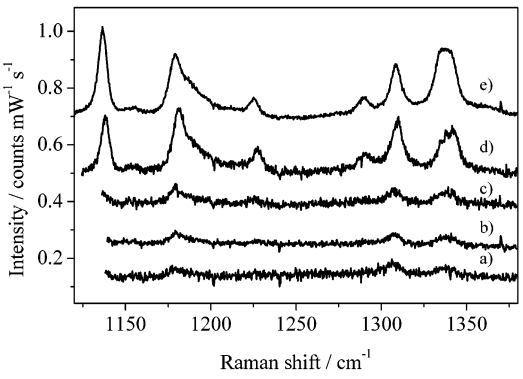

Figure 7. In situ Raman spectra of H_2Pc progressively deposited on a 60-nm-thick PTCDA film, and measured with 647.1-nm excitation in the micro configuration: the H_2Pc thicknesses are (a) 6 nm, (b) 15 nm, (c) 30 nm, and (d) 60 nm. The peak intensity ratios are different when H_2Pc is deposited directly on glass (e).

dissociate the Raman signal from the different layers in the heterostructure using 488.0 nm for PTCDA and 647.1 nm for H_2Pc. Taking advantage of the "transparency" of a wavelength to one of the materials, the first layer of the heterostructure can be probed without interference of overgrowth.

3.3.1. PTCDA/H_2Pc. H_2Pc deposited on top of PTCDA has been shown to depart from the bulk α-H_2Pc herringbone crystal structure and adopts a layered structure where the molecules lie parallel to the substrate and to the PTCDA molecular planes.[4] This modified templated structure is retained through the entire thickness of the H_2Pc film (up to 380 nm) when the PTCDA first layer is more than 15-nm thick.[6] Selective Raman excitation of the H_2Pc component of the heterostructure should be sensitive to its structure; moreover, the deposition of H_2Pc can be followed in situ and any possible relaxation would be detected.

Figure 7 shows in situ resonance Raman spectra recorded after the deposition of an increasing amount of H_2Pc onto a 60-nm PTCDA film. The spectra were all recorded at 647.1 nm and the H_2Pc film thickness ranges from 6 nm (a) to 60 nm (d). There are no significant changes in the frequencies of the main spectral features consistent with no relaxation as the film thickness is increased. Comparison with a H_2Pc film deposited directly on glass (Figure 7e) shows that the peak intensity ratios are affected by the underlying PTCDA layer, indicating structural modification in the double layer. There are no significant shifts in peak position (the error on the peak position is ∼2 cm^{-1}), and any direct chemical interaction between the PTCDA and H_2Pc layers can be excluded. However, the change in the intensity ratios suggests a structural modification in the H_2Pc layer when it is deposited on top of PTCDA.

The intensity ratios of the most intense H_2Pc modes in the PTCDA/H_2Pc heterostructures over the spectral range 400−1540 cm^{-1} are summarized in Table 1 for a H_2Pc thickness of 60 nm. These can be compared to the corresponding values for the 60-nm-thick H_2Pc single layer. The peak intensities are reduced in the heterostructure for the vibrations at 795, 1140, and ∼1340 cm^{-1}, which correspond to macrocycle ring deformations, pyrrole ring deformations, and pyrrole stretching vibrations. Although these vibrations are very delocalized, it is difficult to distinguish any relationship between the observed attenuation and the assignment of the vibration. More importantly, this attenuation is not related to any change in the electronic spectrum, since the vibrations have different excitation profiles (see Figure 3). The changes can only reflect modification of the vibrational properties. Enhanced vibrations are in the region of ring deformations (1197, 1227, and 1290 cm^{-1}), which have a low intensity, or the isoindole C−C stretch at 1533 cm^{-1}. Again, no relation to the excitation profile can be seen. These changes are indicative of a structural modification due to the templating effect of the initial PTCDA layer.

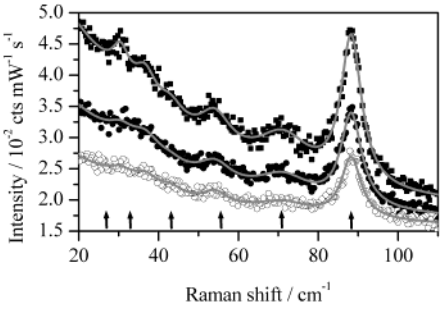

Figure 8. Phonon modes of H_2Pc grown on PTCDA taken in (■) unpolarized, (●) parallel, and (○) crossed-polarized light in micro-Raman configuration. The arrows indicate the positions of the phonons in the H_2Pc single layer, and the fits are superimposed.

Raman can also be used to verify whether the modified structure adopted by H_2Pc on top of PTCDA displays long-range order. Indeed, previous XRD studies on PTCDA/H_2Pc heterostructures showed that the H_2Pc is organized in well-defined planes, but did not give information about the two-dimensional ordering within these planes. A study of the polarization dependence of the vibrational modes and of the phonon modes is therefore crucial to clarify this system.

Micro-Raman studies of the PTCDA/H_2Pc double-layer structure with the 647.1-nm line shows polarization dependence of the H_2Pc internal modes, indicative of an ordered H_2Pc film. Table 1 summarizes the depolarization ratios of the most intense modes and comparison with the depolarization ratios of the H_2Pc single layer shows that the two structures differ.

The Raman spectra shown in Figure 8 for H_2Pc grown on PTCDA show that the second-layer H_2Pc displays phonon modes between 30 and 90 cm^{-1}; these are polarization dependent, indicating long-range ordering. The arrows indicate the positions of the single-layer modes, and Table 2 summarizes the results from the fitting of the phonons in both cases. Above 50 cm^{-1}, the positions of the phonons and the polarization behavior are similar in both the single layer and the heterostructure. However, differences are observed below this threshold. In the heterostructure, two modes are observed at 30 and 37 cm^{-1}, and are hence shifted to higher wavenumber compared to the phonons in the H_2Pc single layer, seen at 26 and 33 cm^{-1}. It is likely that these modes are the most loosely bound, with a small force constant between the molecules. In the heterostructures, these interactions are strengthened, suggesting a stronger overlap in the templated layered structure. This is consistent with the smaller interplanar and intermolecular distances in the templated structure (3.3 Å)[6] as opposed to the single layer (3.4 Å).[31]

The vibrational modes of the underlying PTCDA layer were also probed using 488.0-nm excitation. The PTCDA phonons were measured after progressive H_2Pc deposition, and although the Raman signal was attenuated, no change in the external modes was observed for the range of H_2Pc thicknesses probed. This is further confirmation that H_2Pc does not disrupt the underlying PTCDA structure and that there is no intermixing or diffusion into the PTCDA grains. However it is not possible to assess whether H_2Pc is deposited in the interstitial inter-grain space or only grows on top of the grains. The lack of any modification of PTCDA is again an indication that no chemical bonding takes place between the different materials.

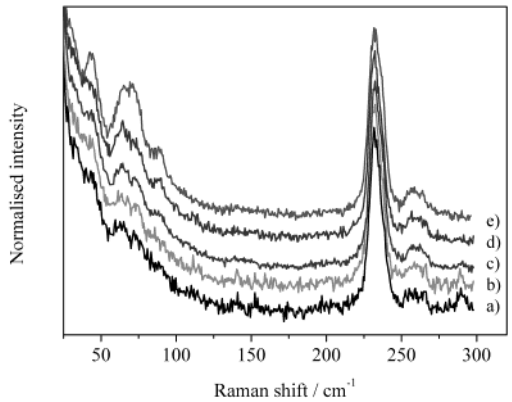

Figure 9. Macro-Raman spectra (taken with the 488.0-nm line) of increasing thicknesses of PTCDA on top of a 60-nm H_2Pc first layer: (a) 6 nm, (b) 12 nm, (c) 18 nm, and (d) 60 nm PTCDA. (e) is a pure 60-nm-thick PTCDA film deposited on a glass substrate. Intensities have been scaled to the internal mode at 233 cm^{-1}.

3.3.2. H_2Pc/PTCDA. PTCDA deposited on top of H_2Pc experiences a strong interaction from the first layer. In structural studies this interaction led to a loss of the X-ray diffraction peak characteristic of PTCDA. However, the origin of the disappearance is still unclear, and could be due to formation of either a microcrystalline, amorphous or templated PTCDA film.

Raman scattering collected on H_2Pc/PTCDA excited at 488.0 nm shows that the position, shape, and intensity of the PTCDA internal modes are unaffected by the H_2Pc underlayer and that the vibration pattern is retained for PTCDA thicknesses between 2 and 60 nm (see Figure 5b). It is important to remember that the intensity of the PTCDA Raman modes saturates after a thickness of ~10 nm (see section 3.2), so that the spectra are representative of a superficial portion of the film. The mode at 233 cm^{-1} displays a Davydov splitting similar to that seen in the single PTCDA layer, suggesting that the intermolecular interactions are similar in both cases. However, the influence of polarization on the peak shape is less pronounced in the heterostructure, indicating a less-ordered structure.

The external modes provide information about the crystallinity of the PTCDA film deposited on top of the H_2Pc layer. Figure 9 shows PTCDA spectra in the phonon region for both the single layer (e), and increasing thicknesses of PTCDA deposited on top of a H_2Pc first layer (a−d). All spectra are normalized to the internal vibration at 233 cm^{-1} so that the intensity of the phonons is independent of film thickness or experimental variations. It can be seen that the intensity of the phonons is about half that expected from the single-layer behavior, indicating the poor crystal quality of PTCDA in a H_2Pc/PTCDA double-layer structure. However, the position of the phonon modes is essentially the same as in unstrained single layers, showing that the structure is identical to bulk PTCDA. The relative intensity of the phonon modes in the heterostructure increases nonlinearly with coverage, indicating a relaxation of the structure as the thickness is increased. The polarization dependence of the phonons is also very weak at low coverages, but increases with film thickness. This again suggests that the PTCDA film undergoes structural relaxation as more material is deposited.

The intensity of the emission from 488.0-nm excitation can be gauged from the background of the Raman spectra at long shifts. It can be seen by comparing the Raman spectra in Figure 5a,b that the luminescence is less intense for PTCDA grown on H_2Pc than in a PTCDA single layer. PL intensity has been correlated to crystal size, and a weak PL is indicative of small crystals.[19] Any reabsorption of the PTCDA emission by H_2Pc is excluded since this would induce an asymmetry in the PL of H_2Pc, which has not been observed.

The PL of PTCDA is centered at ~720 nm, again confirming that the PTCDA top layer has a crystal structure identical to the bulk phase and that emission occurs from deep excimeric traps.[32]

These results indicate that PTCDA adopts a microcrystalline structure when it is deposited on H_2Pc, and that it relaxes progressively to its bulk structure.

4. Conclusions

Raman spectroscopy has been used to probe the crystal quality of single-layer H_2Pc and PTCDA films, through polarization studies and the detection of phonons. The very high selectivity of resonance Raman scattering to the different molecular layers has been used to clarify important issues on the properties of templated double layers based on H_2Pc and PTCDA.

H_2Pc single layers exhibit a strong resonance behavior that can be correlated to their electronic properties. Phonons have been observed for the first time and are an indication of good film crystallinity. Crystal quality is further confirmed by the polarization and geometry dependence of the Raman spectra. Structural order in PTCDA films can also be assessed by the presence of phonons, the strong polarization dependence of external modes, and Davydov splitting of molecular vibrations.

In PTCDA/H_2Pc structures, the relative intensities and polarization dependence of the H_2Pc vibrations are modified with respect to the single layer. Phonon modes are present, although their position is different to those in single layers. This is consistent with a new crystalline structure and supports the layered templated arrangement found by XRD.[4,6] In the case of PTCDA deposited on top of H_2Pc, no modifications to the positions of the vibrations (both internal and external) have been observed. The intensity of the phonons relative to the internal vibrations is greatly attenuated in theses heterostructures. Moreover, the photoluminescence background is also reduced, and has been related to smaller crystal size. These two observations are consistent with the formation of a microcrystalline PTCDA overlayer on top of the initial H_2Pc layer.

The authors gratefully acknowledge the Marie Curie Training Site "Carbon Containing Thin Films" for funding of the collaboration with T. U. Chemnitz, and thank Axel Fechner for technical assistance. S. H. thanks the department of Chemistry, Imperial College, for provision of a teaching assistantship G. S. acknowledges the EU funded Human Potential Research Training Network DIODE (Contract No.: HPRN-CT-1999-00164) for financial support.

References and Notes

(1) Sheats, J. R.; Antoniadis, H.; Hueschen, M.; Leonard, W.; Miller, J.; Moon, R.; Roitman, D.; Stocking, A. *Science* **1996**, *273*, 884.
(2) Forrest, S. R. *Chem. Rev.* **1997**, *97*, 1793.
(3) Tang, C. W. *Appl. Phys. Lett.* **1986**, *48*, 183.
(4) Heutz, S.; Cloots, R.; Jones, T. S. *Appl. Phys. Lett.* **2000**, *77*, 3938.
(5) Bayliss, S. M.; Heutz, S.; Cloots, R.; Middleton, R. L.; Rumbles, G.; Jones, T. S. *Adv. Mater.* **2000**, *12*, 202.
(6) Heutz, S.; Jones, T. S. *J. Appl. Phys.* **2002**, *92*, 3039.
(7) Spiro, G. T.; Li, X.-Y. *Resonance Raman Spectroscopy of Metalloporphyrins*; John Wiley & Sons: New York, 1988.
(8) Aroca, R.; Loutfy, R. O. *J. Raman Spectrosc.* **1982**, *12*, 262.
(9) Aroca, R.; Pieczonka, N.; Kam, A. P. *J. Porphyrins Phthalocyanines* **2001**, *5*, 25.
(10) Aroca, R.; DiLella, D. P.; Loutfy, R. O. *J. Phys. Chem. Solids* **1982**, *43*, 707.
(11) Aroca, R.; Jennings, C.; Loutfy, R. O.; Hor, A.-M. *J. Phys. Chem.* **1986**, *90*, 5255.
(12) Basova, T. V.; Kolesov, B. A. *Thin Solid Films* **1998**, *325*, 140.

(13) Zhao J.; McCreery, R. L. *Langmuir* **1995**, *11*, 4036.
(14) Dowdy, J.; Hoagland, J. J.; Hipps, K. W. *J. Phys. Chem.* **1991**, *95*, 3751.
(15) Kolesov, B. A.; Basova, T. V.; Igumenov, I. K. *Thin Solid Films* **1997**, *304*, 166.
(16) Bayliss, S. M.; Heutz, S.; Rumbles, G.; Jones, T. S. *Phys. Chem. Chem. Phys.* **1999**, *1*, 3673.
(17) Tenne, D. A.; Park, S.; Kampen, T. U.; Das, A.; Scholz, R.; Zahn, D. R. T. *Phys. Rev. B* **2000**, *61*, 14564.
(18) Kaiser, R.; Friedrich, M.; Schmitz-Hubsch, T.; Sellam, F.; Hohenecker, S.; Kampen, T. U.; Leo, K.; Zahn, D. R. T. *Fresenius' J. Anal. Chem.* **1999**, *363*, 189.
(19) Salvan, G.; Tenne, D. A.; Das, A.; Kampen, T. U.; Zahn, D. R. T. *Org. Electron.* **2000**, *1*, 49.
(20) Kampen, T. U.; Tenne, D. A.; Park, S.; Salvan, G.; Scholz, R.; Zahn, D. R. T. *Phys. Status Solidi B* **1999**, *215*, 431.
(21) Scholz, R.; Kobitski, A. Y.; Kampen, T. U.; Schreiber, M.; Zahn, D. R. T.; Jungnickel, G.; Elstner, M.; Sternberg, M.; Frauenheim, T. *Phys. Rev. B* **2000**, *61*, 13659.
(22) Kam, A. P.; Aroca, R.; Duff, J. *Chem. Mater.* **2001**, *13*, 4463.
(23) Heutz, S.; Bayliss, S. M.; Middleton, R. L.; Rumbles, G.; Jones, T. S. *J. Phys. Chem. B* **2000**, *104*, 7124.
(24) Yim, S.; Heutz, S.; Jones, T. S. *J. Appl. Phys.* **2002**, *91*, 3632.
(25) Bovill, A. J.; McConnell, A. A.; Nimmo, J. A.; Smith, W. E. *J. Phys. Chem. B* **1986**, *90*, 569.
(26) Albrecht, A. C. *J. Chem. Phys.* **1961**, *34*, 14761.
(27) Myers, A. B.; Mathies, R. A. *Resonance Raman Intensities: A Probe of Excited-State Structure and Dynamics*; John Wiley & Sons: New York, 1987.
(28) Tackley, D. R.; Dent, G.; Smith, W. E. *Phys. Chem. Chem. Phys.* **2001**, *3*, 1419.
(29) Leznoff, C. C.; Lever, A. B. P. *Phthalocyanines−Properties and Applications*; VCH: New York, 1989−1996.
(30) Kampen, T. U.; Salvan, G.; Tenne, D. A.; Scholz, R.; Zahn, D. R. T.; *Appl. Surf. Sci.* **2001**, *175−176*, 326.
(31) Janczac, J.; Kubiac, R. *J. Alloys Compd.* **1992**, *190*, 121.
(32) Heutz, S.; Ferguson, A.; Rumbles, G.; Jones, T. S. *Org. Electron.* **2002**, *3*, 119.